Results in Physics 8 (2018) 468–472

Contents lists available at ScienceDirect

Results in Physics

journal homepage: www.journals.elsevier.com/results-in-physics

A self-powered nano-photodetector based on PFH/ZnO nanorods organic/inorganic heterojunction

Xiaoyun Li, Wei Liu, Peigang Li *, Jia Song, Yuehua An, Jingqin Shen, Shunli Wang, Daoyou Guo *

Department of Physics, Center for Optoelectronic Materials and Devices, Zhejiang Sci-Tech University, Hangzhou 310018, PR China

ARTICLE INFO

Article history:
Received 27 October 2017
Received in revised form 10 December 2017
Accepted 12 December 2017
Available online 15 December 2017

ABSTRACT

PFH/ZnO nanorods heterojunctions were fabricated by spin-coating *p*-type Poly (9,9-dihexylfluorene) (PFH) on n-type vertically aligned ZnO nanorod arrays grown by a facile hydrothermal method on indium tin oxide (ITO) transparent conductive glass. A typical *p-n* junction behavior was observed in the fabricated heterojunction. The current of heterojunction increases and decreases dramatically by switching the illumination on and off at zero bias, showing potential self-powered photodetector applications. The heterojunction were capable of generating negative current when illuminated under an appropriate wavelength. The photoresponse properties of the heterojunction can be tuned by the applied bias. In vacuum, the rectifying behavior disappeared, and show only simple semiconductor behavior. Band structure of the heterojunction was schematic drawn and explain the mechanism of the properties of PFH/ZnO nanorods heterojunctions.

Organic/inorganic semiconductor hybrid structures have received much attention from researchers because of their unique properties resulted from the combination of two type of materials, thereby allowing such structures to be used in novel devices design and leading to many practical applications [1–4]. Among inorganic semiconductor materials, ZnO has been extensively investigated and demonstrated its capability of constructing high quality optoelectronic devices, especially in the ultraviolet detectors due to its wide band gap of 3.37 eV [5,6]. *P-n* junction is an important component to construct optoelectronic device, e.g. photodetector, solar cell, and light emitting diode. It has been demonstrated that it's difficult to experimentally obtain a stable *p*-type ZnO, so it would be great to find a suitable *p*-type semiconductor to construct *p-n* junction with ZnO. Organic semiconductors have many advantages, such as high absorption coefficient, variable bandwidth, low cost and excellent manufacturing performance [7,8]. Pure organic or inorganic semiconductor materials have their own advantages and disadvantages, and their own shortages limit the scope of their applications. Organic/inorganic semiconductor heterojunctions can make full use advantages of the organic component's excellent processability and inorganic component's efficient carrier migration ability; such hybrid structure might produce some novel excellent performance. In this paper, we fabricated ZnO nanorods based organic/inorganic *p-n* junction, and studied the properties of the structure.

Vertically aligned ZnO nanorods were grown by a facile hydrothermal method on indium tin oxide (ITO) transparent conductive glass [9], and PFH/ZnO heterojunction structure were fabricated using spin coating a sol of poly (9,9-dihexylfluorene) (PFH) in chloroform on ZnO nanorods films with a speed of 3000 rpm for 40 s [10]. Then, 50-nm-thick Au electrodes in size of 1.5 mm × 1.5 mm, defined by a shadow mask, were evaporated onto the active layer using magneto sputtering technique under vacuum of $\sim 10^{-4}$ Pa.

The crystal structure of ZnO nanorods were characterized by X-ray powder diffraction (XRD). The morphology of ZnO nanorods and the cross-sections of PFH/ZnO heterojunctions were examined by a Hitachi S-4800 field emission scanning electron microscope (SEM). UV-Vis absorption spectra of ZnO nanorods and PFH were acquired using a Varian Cary 50 conc UV-Visible spectrophotometer. The photoluminescence (PL) spectra were taken on a Hitachi F-7000 spectrofluorimeter equipped with a 150 W Xenon lamp and 1–3 kV electron beam (self-made electron gun, 10^{-6} Pa vacuum, filament current 102.5 mA) as the excitation source and the excitation wavelength was set to 325 nm.

The current-voltage (*I-V*), time dependent (*I-t*) photoresponse of the fabricated devices were measured using a Keithley 2400 source-meter in a two-probe configuration. For the photoelectrical properties measurement, a 405 nm blue laser with a power of 150 mW, a 365 nm and a 254 nm bulb with power of 6 W were used as

* Corresponding authors.
E-mail addresses: pgli@zstu.edu.cn (P. Li), dyguo@zstu.edu.cn (D. Guo).

https://doi.org/10.1016/j.rinp.2017.12.031
2211-3797/

light source. The temperature dependent electrical transport properties were measured on a home-made low temperature measurement system.

Fig. 1a shows a typical SEM image of single crystalline ZnO nanorods array with orientation preferentially vertical to the ITO substrate. Fig. 1b shows a magnified SEM image of the grown ZnO nanorods array. The average diameter is ~70 nm. Fig. 1c shows the XRD patterns of ZnO nanorods array on the substrate. The diffraction peaks of the ZnO nanorods in ITO/ZnO are agree well with the hexagonal wurtzite structure (JCPDS file No. 36-1451). The predominant (0 0 2) peak shows the preferential orientation growth of the ZnO NRAs along [0 0 0 1] direction, which is consistent with the SEM observation in Fig. 1b. Fig. 1d shows the cross-sectional SEM image of the PFH/ZnO nanorods heterojunction structure. We can see that the length of nanorods is ~1 μm. Fig. 1e and f shows the absorption and PL spectra of the ZnO nanorods and PFH. For the ZnO nanorods, the fundamental absorption edge is located in the UV region of 380 nm. The PL spectra exhibit a strong UV emission peak at ~350 nm, which is related to the near-band edge emission of the wide band gap ZnO. An additional blue band at 400–500 nm is observed as well, which is mainly caused by the intrinsic defects or oxygen vacancies in ZnO [11]. For PFH, a broad absorption spectrum ranged from 300 to 425 nm with a peak at about 382 nm is observed. The PL spectrum of PFH shows a broad emission range with two distinct peaks at 428 and 44 nm, respectively.

In order to study the photosensitivity of the PFH/ZnO heterojunction, the light sources with the wavelengths of 254 nm, 365 nm and 405 nm were used to illuminate the device. The inset of Fig. 2a shows the schematic diagram of the ZnO/PFH heterojunction structure. Fig. 2a shows the *I-V* characteristics of ZnO/PFH heterojunction under dark and illumination of 254 nm, 365 nm and 405 nm at room temperature in air. The *I-V* characteristics show the rectifying behavior and an obvious photoresponse, which can be attributed to the formation of *p-n* junction between *p*-typed PFH and the *n*-typed ZnO nanorods [12–14]. Fig. 2b shows the ratio

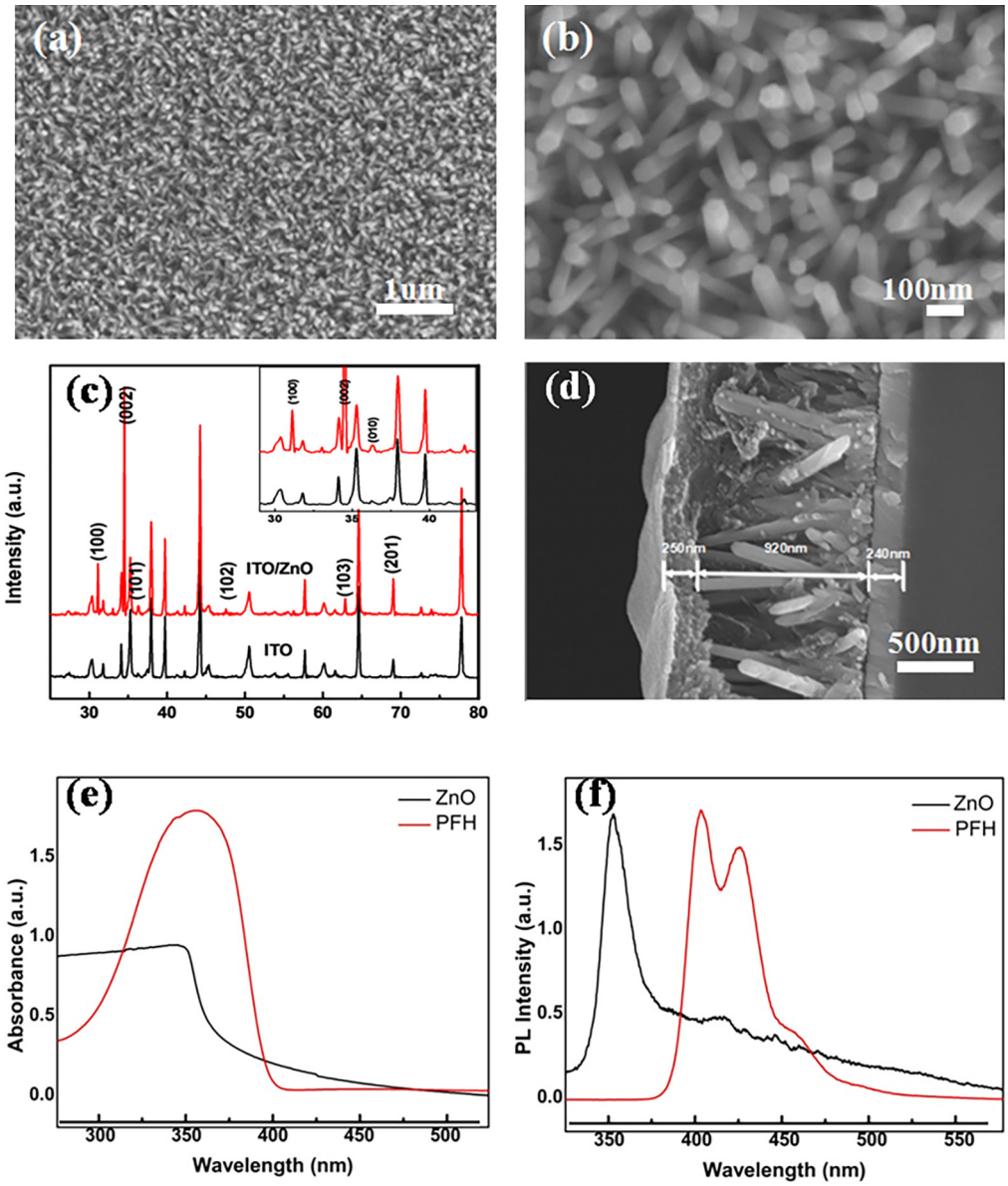

Fig. 1. a) The top view of SEM image of ZnO nanorods, b) An magnified SEM image of grown ZnO nanorods, c) X-ray diffraction patterns for ZnO nanorods array, d) The cross-sectional SEM image of the PFH/ZnO heterojunction structure, e) The absorption spectra and f) The PL spectra of ZnO nanorods and PFH.

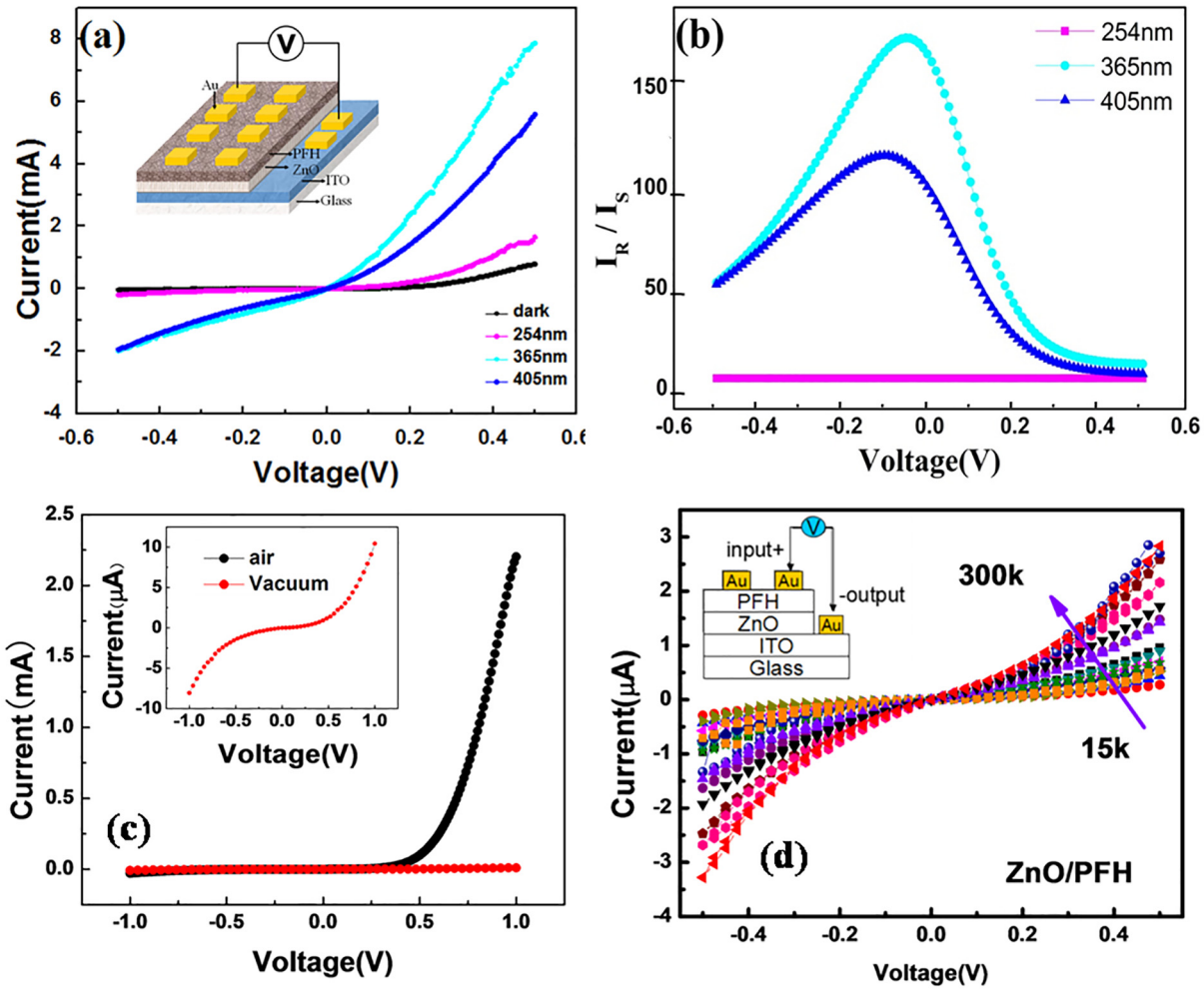

Fig. 2. a) The *I-V* characteristics of PFH/ZnO heterojunction under dark and illuminated with 254 nm, 365 nm, 405 nm light in room temperature. Inset shows the schematic diagram of the heterojunction test method, b) The current ratio between photocurrent and dark current at different voltage under 254 nm, 365 nm and 405 nm light illuminated, c) The *I-V* characteristics of PFH/ZnO heterojunction in air and vacuum under dark, d) The *I-V* characteristics of PFH/ZnO heterojunction at different temperature in the range of 15–300 K.

between photocurrent and dark current at different voltage. The maximum ratio is not at 0 V, which may be related to the bias tuning depletion layer thickness of heterojunction. In order to measure the electrical transport properties, the device was put in vacuum, we found that the resistance of the device in vacuum was much larger than that in air (shown in Fig. 2c). Fig. 2d shows the *I-V* curves at different temperature in the range of 15–300 K. It is shown that the resistance of the device increases with the decrease of temperature.

Fig. 3a and b show the *I-t* characteristics of the PFH/ZnO heterojunction under the light illumination with the different wavelengths of 254 nm and 365 nm. The current of heterojunction slightly increases when the light turns on while the current decreases while that turns off at 0 V bias, exhibiting a self-powered characteristic [15,16]. The negative current was observed with a bias of 0 V for the illumination of 405 nm light, which can return to 0 A at dark. Such phenomenon will disappear if we applied a tiny bias on the heterostructure, as is shown in Fig. 3d. This interesting phenomenon may be related to the built-in electric field and Schottky barrier, the specific mechanism remains to be further studied.

The opto-electrical transport properties in air should be related to the energy band structure of PFH/ZnO heterojunction. The schematic energy band diagram of PFH/ZnO heterojunction is shown in Fig. 3e. The band gaps of ZnO nanorods (E_g) and PFH (E_g) are 3.4 eV and 3.1 eV respectively. Under the light illumination, the electron-hole pairs were generated in PFH and ZnO respectively. For PFH, the photogenerated carriers are with electrons injecting into the lower unoccupied molecular orbital and holes leaving in the highest occupied molecular orbital. For ZnO, the photogenerated carriers are mainly with electrons injecting into the conduction band and holes leaving in valence band. The photogenerated electron-hole pairs in the depletion region will separate by potential barrier and subsequently transport toward corresponding electrodes for the 0 V bias. As a result, the photocurrent was produced, and the PFH/ZnO heterojunction shows a self-powered photodetection characteristic.

In summary, ZnO nanorods array films were grown using simple hydrothermal method, and organic/inorganic *p-n* heterojunctions were fabricated by spin-coating *p*-type organic materials PFH on the grown ZnO nanorods thin films. A typical *p-n* junction behavior, rectifying characteristics in current-voltage *I-V* curves, was observed. The heterojunction can be turned "on" and "off" reversibly by switching the illumination on and off. Such organic/inorganic heterojunction can be used to fabricate a self-powered nano-photodetector. When illuminated

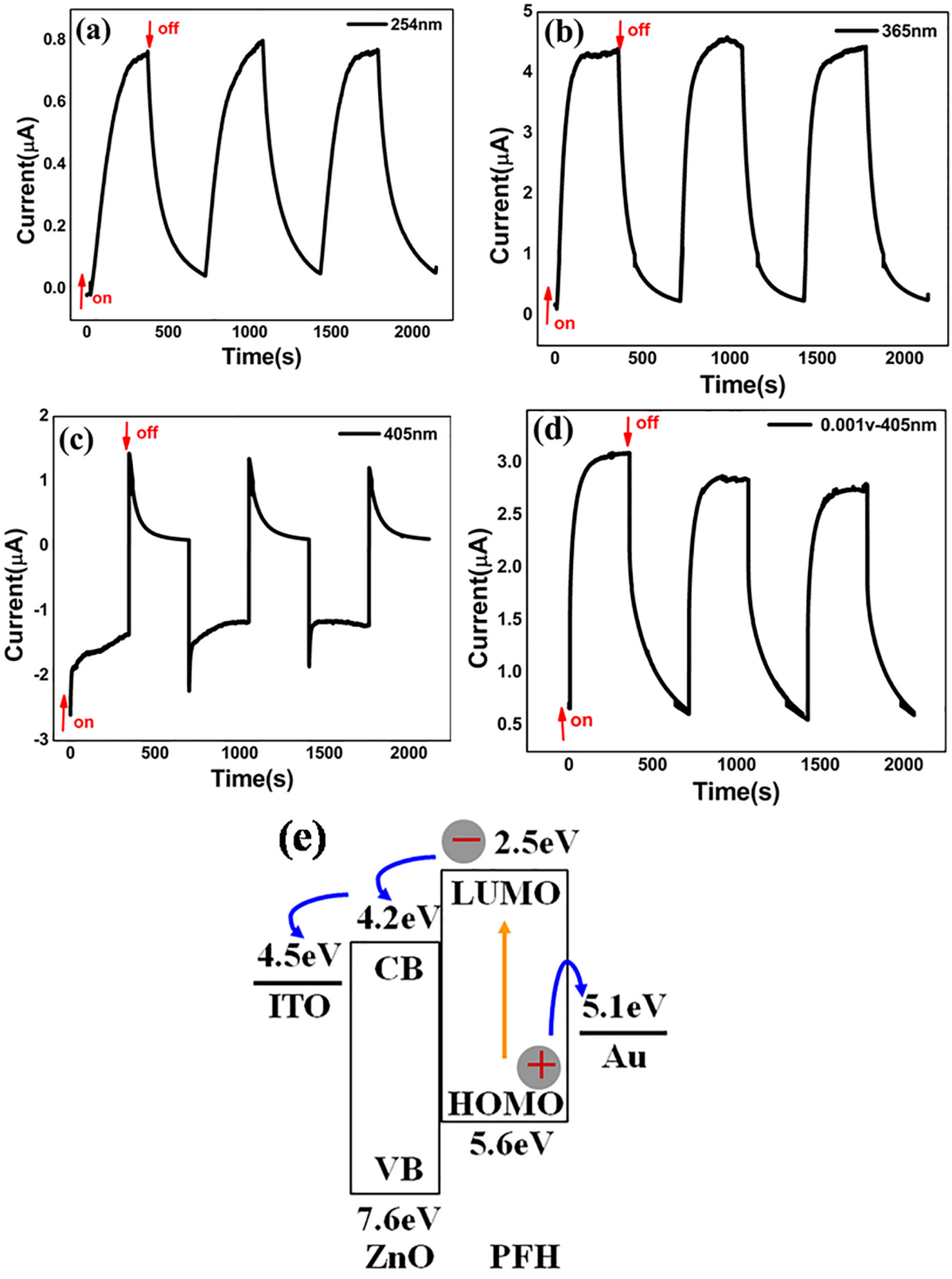

Fig. 3. The *I-t* characteristics of the PFH/ZnO heterojunction at 0 V bias illuminated with light sources in wavelengths of a) 254 nm, b) 365 nm and c) 405 nm, d) The *I-t* characteristics of the PFH/ZnO heterojunction with applied 0.001 V reverse bias, e) Schematic energy band diagram for PFH/ZnO heterojunction.

with an appropriate wavelength, opposite current will generate. The process used to fabricate device in this presentation could be a promising alternative to fabricate the low-cost photodetector for its compatible to large area and flexible substrate technique.

Acknowledgements

The authors would like to acknowledge financial support from the National Natural Science Foundation of China (No. 61704153, 61774019), the Scientific Research Project for the Education Department of Zhejiang Province (No. Y201738294), Science and Technology Department of Zhejiang Province Foundation (Grant No. 2017C37017).

References

[1] Shao D, Yu M, Sun H, et al. ACS Appl Mater Inter 2014;6:14690.
[2] Vaynzof Y, Kabra D, Zhao L, et al. Appl Phys Lett 2010;97:033309.
[3] Chang JA, Rhee JH, Im SH, et al. Nano Lett 2010;10:2609.
[4] Wang X, Wang Y, Liu G, et al. Dalton T 2011;40:9299.
[5] Reyes PI, Ku CJ, Duan Z, et al. Appl Phys Lett 2012;101:031118.
[6] Yang S, Tongay S, Li SS, et al. Appl Phys Lett 2013;103:143503.
[7] Mei J, Diao Y, Appleton AL, et al. J Am Chem Soc 2013;135:6724.
[8] Gélinas S, Rao A, Kumar A, et al. Science 2014;343:512.
[9] Vayssieres L. Adv Mater 2003;15:464.
[10] Li HG, Wu G, Chen HZ, et al. Curr Appl Phys 2011;11:750.
[11] Bardhan R, Wang H, Tam F, et al. Langmuir 2007;23:5843.
[12] Look DC, Coskun C, Claflin B, et al. Physica B: Condens Matter 2003;340:32.
[13] Li HG, Wu G, Shi MM, et al. Appl Phys Lett 2008;93:153309.
[14] Mridha S, Basak D. Appl Phys Lett 2008;92:142111.
[15] Guo DY, Liu H, Li PG, et al. ACS Appl Mater Interfaces 2017;9:1619.
[16] Li PG, Shi HZ, Chen K, et al. J Mater Chem C 2017;5:10562.